Thermodynamics of the Complex Protein Unfolding Reaction of Barstar†

Vishwas R. Agashe,‡ Franz X. Schmid,§ and Jayant B. Udgaonkar*,‡

National Centre for Biological Sciences, Tata Institute of Fundamental Research Centre, Post Office Box 1234, Indian Institute of Science Campus, Bangalore 560012, India, and Laboratorium für Biochemie, Universität Bayreuth, D-95440 Bayreuth, Germany

Received May 7, 1997; Revised Manuscript Received August 4, 1997⊗

ABSTRACT: The complex unfolding reaction of barstar has been characterized by studying the apparent rate of unfolding, monitored by intrinsic Trp fluorescence, as a function of temperature and guanidine hydrochloride (GdnHCl) concentration. The kinetics of unfolding and folding of wild-type (wt) barstar at 5 °C were first studied in detail. It is shown that when unfolding is carried out using concentrations of GdnHCl in the posttransition zone of unfolding, the change in fluorescence that accompanies unfolding occurs in two phases: 30% of the change occurs in a burst phase that is complete within 4 ms, and 70% of the change occurs in a fast phase that is complete within 2 s. In contrast, when the protein is unfolded at 25 °C, no burst-phase change in fluorescence is observed. To confirm that a burst-phase change in fluorescence indeed accompanies unfolding at low temperature, unfolding studies were also carried out on a marginally destabilized mutant form of barstar for which the burst-phase change in fluorescence is shown to be as high as 70%. These results confirm a previous report [Nath *et al.*, (1996), *Nat. Struct. Biol. 3*, 920−923], in which the detection of a burst-phase change in circular dichroism at 222 nm during unfolding at 25 °C led to the inclusion of a rapidly formed kinetic intermediate, I_U, on the unfolding pathway. To characterize thermodynamically the unfolding pathway, apparent unfolding rates were then measured at six different concentrations of GdnHCl in the range 2.6 to 5.0 M, at five different temperatures from 5 to 46 °C. The subsequent analysis was done on the basis of the observation that a preequilibrium between the fully folded state (F) and I_U gets established rapidly before further unfolding to the completely unfolded state (U). The results indicate that I_U has a specific heat capacity similar to that of F and therefore suggest that I_U is as compact as F, with practically no exposure of the hydrophobic core. On the other hand, the transition state of unfolding has a 45% greater heat capacity than F, indicating that significant hydration of the hydrophobic core occurs only after the rate-limiting step of unfolding.

Characterization of the transition state of folding remains a major goal of protein folding studies. The transition state is a high-energy metastable state and thus requires the use of indirect methods to elucidate its structure. Traditional approaches rely on studying the effect of a systematic variation in temperature and denaturant concentration on the folding and unfolding kinetics of the protein (Chen *et al.*, 1989; Chen & Matthews, 1994; Schindler & Schmid, 1996). The advent of pragmatic mutagenesis or the "protein engineering approach", coupled with the traditional approach, has provided a means to infer the structural attributes of these ephemeral states in greater detail (Matouschek *et al.*, 1989; Fersht, 1995a,b).

Kinetically well characterized proteins are good systems to use for such studies. Barstar (Figure 1), the 89 residue, intracellular inhibitor of barnase, is one such protein. The folding and unfolding transitions of barstar have been studied extensively using both equilibrium (Khurana & Udgaonkar, 1994; Khurana *et al.*, 1995; Agashe & Udgaonkar, 1995; Wintrode *et al.*, 1995) and kinetic methods (Schreiber & Fersht, 1993; Shastry *et al.*, 1994; Shastry & Udgaonkar, 1995; Agashe *et al.*, 1995; Nath *et al.*, 1996; Nölting *et al.*, 1995, 1997).

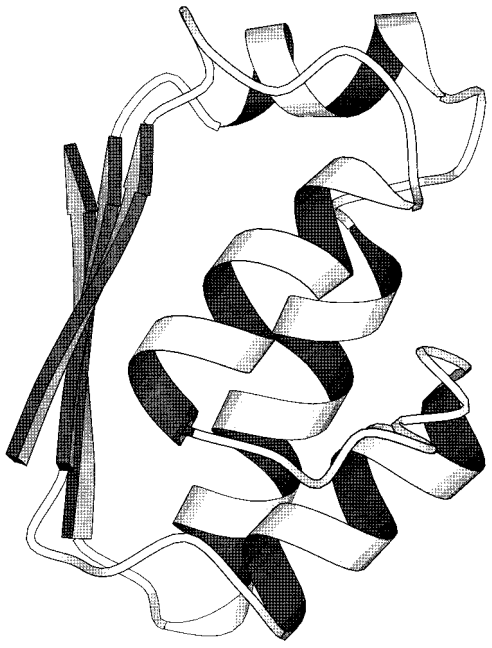

FIGURE 1: Solution structure of barstar. The figure was drawn using Molscript (Kraulis, 1981).

Equilibrium studies established that barstar has unusual thermodynamic properties for a protein of its size (Agashe & Udgaonkar, 1995). It has an unusually high denaturational

† This work was funded by the Tata Institute of Fundamental Research and the Department of Biotechnology, Government of India.

* Corresponding author: E-mail jayant@ncbs.tifrbng.res.in.

‡ National Centre for Biological Sciences.

§ Universität Bayreuth.

⊗ Abstract published in *Advance ACS Abstracts,* September 15, 1997.

S0006-2960(97)01062-3 CCC: $14.00

heat capacity increment, ΔC_p, on unfolding (16.4 cal·mol^{-1}·K^{-1} per residue), myoglobin being the only other protein known with a higher value (18 cal·mol^{-1}·K^{-1} per residue). The enthalpy change, ΔH, on unfolding barstar at room temperature, on the other hand, is unusually small (4 kcal·mol^{-1}) and so is the entropy change (as a consequence). The high ΔC_p value in conjunction with the small ΔH leads to a higher susceptibility to cold denaturation, which has been demonstrated convincingly (Agashe & Udgaonkar, 1995). Wintrode *et al.* (1995) have theoretically deconvoluted the overall ΔH of barstar unfolding into the ΔH of hydration and ΔH of internal interactions. They concluded that while the ΔH of hydration is comparable to other proteins, the ΔH of internal interactions is unusually low and accounts for the low value of the overall ΔH of unfolding. Bovine pancreatic trypsin inhibitor (BPTI) is the only other protein to have a lower value for the ΔH of internal interactions (Wintrode *et al.*, 1995).

Kinetic studies on barstar have shown the presence of multiple pathways and multiple intermediates (Schreiber & Fersht, 1993; Shastry & Udgaonkar, 1995). The unfolded state, U, of barstar is kinetically heterogeneous, containing fast-folding, U_F, and slow-folding, U_S, species (Schreiber & Fersht, 1993; Shastry *et al.*, 1994). U_F molecules have the Tyr47-Pro48 bond in the "native" *cis* conformation, while the U_S molecules have this bond in the "nonnative" *trans* conformation. Barstar unfolding has been shown to follow the extended two-state model, $F \rightleftharpoons U_F \rightleftharpoons U_S$, in the transition and the posttransition zone of equilibrium unfolding (Shastry *et al.*, 1994). Recent studies on barstar revealed the presence of a kinetic intermediate, I_U, on the unfolding pathway (Nath *et al.*, 1996). I_U is a burst-phase intermediate that forms within 4 ms, which lacks a considerable amount of the native secondary structure but possesses a nonhydrated hydrophobic core (Nath *et al.*, 1996).

Almost all proteins studied have been reported to unfold in simple monophasic processes that reflect the existence of a single transition state or a set of energetically similar transition states. Barstar and a few other proteins (Laurents & Baldwin, 1997; Kiefhaber *et al.*, 1995; Hoeltzli & Frieden, 1995) that unfold via an intermediate are exceptional in possessing more complex unfolding kinetics. Current understanding of the role of unfolding intermediates and their structural attributes is very poor. It is therefore an attractive proposition to study the thermodynamics of the unfolding process and obtain structural information about such intermediates as well as the transition states separating them from the completely unfolded state.

This paper describes the folding and unfolding kinetics of barstar at a low temperature (5 °C) and presents a thermodynamic analysis of the unfolding kinetics using the traditional approach. The kinetic data at 5 °C reveal directly the presence of the intermediate I_U during unfolding, using intrinsic Trp fluorescence as a probe. The inclusion of an intermediate in the unfolding scheme used for the thermodynamic analysis has allowed additional information about the structural attributes of this intermediate and the transition state of unfolding to be obtained. Specifically, it is shown that I_U is similar to F by the heat capacity criterion, while the transition state, TS, is only 55% nativelike. It is inferred that while partial hydration of the hydrophobic core occurs during initial unfolding to I_U at low temperature, complete penetration of water into the hydrophobic core of the protein occurs only during the rate-limiting step in unfolding.

MATERIALS AND METHODS

Materials. GdnHCl[1] was of the highest purity grade from Sigma Chemical Co. All other chemicals including the buffer components were also of the highest purity grade from Merck (Germany).

Protein Purification. The procedure for the purification of wt barstar has been described previously (Khurana & Udgaonkar, 1994) and was used without change. The purification procedure for the W38FW44F mutant protein is the same as that for the wild-type protein (Nath & Udgaonkar, 1997). The yield of both these proteins was close to 200 mg/L of cell growth.

Data Collection. Data were acquired in 20 mM sodium phosphate buffer at pH 8.0 containing 50 μM EDTA and 0.1 mM DTT, at all temperatures. Solutions were passed through 0.45 μm Corning filters and degassed before use.

Kinetic Experiments. A DX.17 MV sequential mixing stopped-flow spectrometer from Applied Photophysics (Leatherhead, U.K.) was used for the experiments done at 5 °C. The path length of the chamber was 2 mm and a 320 ± 10 nm band-pass filter from Oriel Corp. was used in the detection path. The folding/unfolding kinetics were thus followed with excitation at 287 nm and detection at 320 nm. The typical protein concentration used in the observation chamber was 7 μM, reached after a 1:5 dilution of the protein stock in the appropriate buffer (native or unfolding). The manual-mixing experiments with identical excitation and emission wavelengths, for folding and unfolding at 5 °C, were performed on a Hitachi F-4010 spectrofluorometer with an integrated magnetic stirrer. The fluorometer was interfaced to a computer and data collection was performed continuously for the first 240 s, and later points were taken every 60 s. These later points were an average of the fluorescence intensity measured over a period of 8 s. Between data collection the excitation shutter was closed to minimize bleaching of the sample.

Kinetic unfolding experiments done at 10 °C with the W38FW44F mutant of barstar were performed on a Biologic (Cedex, France) SFM-3 sequential mixing stopped-flow instrument. The excitation wavelength was set at 295 nm. The FC-15 cuvette used had a path length of 1.5 mm, and a 320 ± 10 nm band-pass filter from Oriel was used in the detection path.

Equilibrium experiments. Equilibrium unfolding experiments on the wild-type protein at 5 °C were also performed on the Hitachi F-4010 spectrofluorometer. The excitation slit width was set at 3 nm, while that for emission was set at 10 nm.

Data Analysis: (a) Isothermal GdnHCl-Induced Unfolding Curves. Equilibrium GdnHCl-induced unfolding curves were analyzed to obtain ΔG_{FU}, the free energy of unfolding in water by fitting the data to a two-state $F \rightleftarrows U$ unfolding model, using a nonlinear least-squares fitting routine as described previously (Agashe & Udgaonkar, 1995).

[1] Abbreviations: GdnHCl, guanidine hydrochloride; CD, circular dichroism; DTT, dithiothreitol; EDTA, ethylenediaminetetraacetic acid; wt barstar, wild-type barstar; W38FW44F, the double mutant of barstar where the side chains Trp38 and Trp44 have been mutated to phenylalanines.

(b) Kinetic Studies. The observable kinetics of folding of barstar are described by a two-exponential process (Shastry *et al.*, 1994):

$$A(t) = A(\infty) - A_1 \exp(-\lambda_1 t) - A_2 \exp(-\lambda_2 t) \quad (1)$$

λ_1 and λ_2 are the apparent rate constants of the slow and fast phases, and A_1 and A_2 are the respective amplitudes. The relative amplitude of the slow phase, α_1, was determined by dividing the amplitude of the observed slow phase by the equilibrium amplitude of the reaction at that GdnHCl concentration. At 5 °C, where λ_2 is more than 5000 times faster than λ_1, the fast phase of folding was fit to a single exponential: eq 1 was used with A_1 set to 0.

The observable kinetics of unfolding in the transition region are also described by a two-exponential process:

$$A(t) = A(\infty) + A_1 \exp(-\lambda_1 t) + A_2 \exp(-\lambda_2 t) \quad (2)$$

The observable kinetics of unfolding in the posttransition region are described by a single-exponential process: eq 2 was used with A_1 set to 0.

(c) Temperature and GdnHCl-Dependence of the Folding and Unfolding Kinetics. The kinetics of unfolding of barstar are described by the following mechanism (Nath *et al.*, 1996):

$$F \overset{K_{FI}}{\rightleftharpoons} I_U \xrightarrow{k_{IU}} U \quad (3)$$

In this mechanism, fully folded protein F unfolds very rapidly to the partly unfolded intermediate, I_U, which unfolds more slowly to completely unfolded protein U.

When the transition between F and I_U is much faster than that from I_U to U, a rapid preequilibrium is established between F and I_U, characterized by the equilibrium constant K_{FI} . The observed rate of unfolding, λ_2, is related to the microscopic rate constant k_{IU} by

$$\lambda_2 = \frac{K_{FI}}{1 + K_{FI}} k_{IU} \quad (4)$$

A similar relation was used for analyzing the folding of ubiquitin and barnase, both of which fold via a rapidly formed folding intermediate (Khorasanizadeh *et al.*, 1996; Oliveberg *et al.*, 1995).

The temperature dependence of K_{FI} is described by

$$K_{FI} = \exp\left(\frac{-\Delta G_{FI}(T)}{RT}\right) \quad (5)$$

R is the universal gas constant. ΔG_{FI} is free energy difference between F and I_U and can be described in terms of the corresponding differences in enthalpy, ΔH_{FI}, entropy, ΔS_{FI}, and heat capacity $\Delta C_{p,FI}$.

The change in free energy that occurs on unfolding of F to I_U in the presence of denaturant, denoted here by $\Delta G'_{FI}$, is assumed to have a linear dependence on the concentration of denaturant, [D] (Schellman, 1987; Agashe & Udgaonkar, 1995):

$$\Delta G'_{FI} = \Delta G_{FI} + \Delta G_{FI}^{i}[D] \quad (6)$$

ΔG_{FI}^{i}, is the change in free energy associated with the preferential interaction of denaturant with I_U rather than F. Similarly, the corresponding changes in enthalpy, entropy, and heat capacity, denoted by $\Delta H'_{FI}$, $\Delta S'_{FI}$, and $\Delta C'_{p,FI}$, respectively, are also assumed to have linear dependences on [D]. ΔH_{FI}^{i}, ΔS_{FI}^{i}, and $\Delta C_{p,FI}^{i}$ represent the changes in enthalpy, entropy, and heat capacity, respectively, that describe ΔG_{FI}^{i}.

The temperature dependence of $\Delta G'_{FI}$ is therefore given by

$$\Delta G'_{FI}(T) = \Delta H'_{FI}(T^0) - T\Delta S'_{FI}(T^0) + \Delta C'_{p,FI}\left(T - T^0 - T \ln \frac{T}{T^0}\right) \quad (7)$$

T^0 is the standard reference temperature, taken here as 25 °C. $\Delta H'_{FI}(T^0)$ and $\Delta S'_{FI}(T^0)$ are the values of $\Delta H'_{FI}$ and $\Delta S'_{FI}$ at T^0. $\Delta C'_{p,FI}$ is assumed to be independent of temperature in the temperature range studied (5−46 °C).

The temperature dependence of k_{IU} is described by the Eyring equation (Atkins, 1978):

$$k_{IU} = \frac{k_B T \kappa}{h} \exp\left(\frac{\Delta G_{IU}^{\ddagger}(T)}{RT}\right) \quad (8)$$

where k_B and h are the Boltzmann and Planck constants, respectively. The transmission coefficient, κ, has been set arbitrarily equal to 1, because there is no way to estimate its value for protein folding transitions (Hänggi, 1990). $\Delta G_{IU}^{\ddagger}$ is the activation free energy of unfolding and corresponds to the Gibbs free energy difference between I_U and the transition state (TS) of the $I_U \rightarrow U$ reaction, which is also the transition state of the overall unfolding reaction. $\Delta G_{IU}^{\ddagger}$ can be described in terms of the enthalpy of activation, $\Delta G_{IU}^{\ddagger}$, the entropy of activation, $\Delta S_{IU}^{\ddagger}$, and the heat capacity difference between I_U and U, $\Delta C_{p,IU}^{\ddagger}$.

The change in free energy, $\Delta G'_{IU}{}^{\ddagger}$, that occurs upon activation from I_U to TS in the presence of denaturant is also assumed to have a linear dependence on [D]:

$$\Delta G'_{IU}{}^{\ddagger} = \Delta G_{IU}{}^{\ddagger} + \Delta G_{IU}{}^{\ddagger,i}[D] \quad (9)$$

$\Delta G_{IU}^{\ddagger,i}$ is the change in free energy associated with the preferential interaction of denaturant with the TS rather than I_U. Similarly, the corresponding enthalpy, entropy, and heat capacity, denoted by $\Delta H'_{IU}{}^{\ddagger}$, $\Delta S'_{IU}{}^{\ddagger}$, and $\Delta C'_{p,IU}{}^{\ddagger}$, respectively, are also assumed to have a linear dependence on [D]. $\Delta H_{IU}^{\ddagger,i}$, $\Delta S_{IU}^{\ddagger,i}$, and $\Delta C_{p,IU}^{\ddagger,i}$ are the enthalpy, entropy, and heat capacity, respectively, that describe $\Delta G_{IU}^{\ddagger,i}$.

The temperature dependence of $\Delta G'_{IU}{}^{\ddagger}$ is therefore given by

$$\Delta G'_{IU}{}^{\ddagger}(T) = \Delta H'_{IU}{}^{\ddagger}(T^0) - T\Delta S'_{IU}{}^{\ddagger}(T^0) + \Delta C'_{p,IU}{}^{\ddagger}\left(T - T_0 - T \ln \frac{T}{T^0}\right) \quad (10)$$

T^0 is the standard reference temperature, taken here as 25 °C. $\Delta H'_{IU}{}^{\ddagger}(T^0)$ and $\Delta S'_{IU}{}^{\ddagger}(T^0)$ are the values of $\Delta H'_{IU}{}^{\ddagger}$ and $\Delta S'_{IU}{}^{\ddagger}$ at T^0. $\Delta C_{p,IU}^{\ddagger}$ is assumed to be independent of temperature in the temperature range studied (5−46 °C).

The dependence of λ_2 on temperature and denaturant concentration is therefore given by

$$\lambda_2 = \frac{k_B T}{h}\left(\frac{e^{-\Delta G'_{FI}/RT}}{1 + e^{-\Delta G'_{FI}/RT}}\right) e^{-\Delta G'_{IU}{}^{\ddagger}/RT} \quad (11)$$

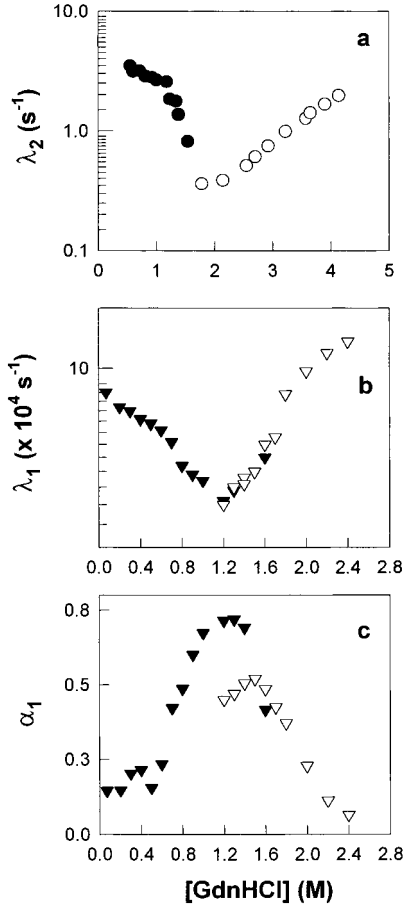

FIGURE 2: Kinetics of folding and unfolding of barstar at pH 8, 5 °C. Empty and filled symbols represent data obtained from unfolding and folding experiments, respectively. (○, ●) data obtained from stopped-flow mixing experiments. (▽, ▼) Data obtained from manual mixing experiments. (a) Rate constant of the fast phase in folding and unfolding, λ_2. Each point is an average of at least eight separate traces. (b) Rate constant of the slow phase in folding and unfolding, λ_1. (c) Relative amplitude of the slow phase, α_1. Each point is an average of at least three separate experiments. All measurements had a standard deviation of ±10%.

where the dependence of $\Delta G'_{FI}$ on temperature and denaturant concentration is given by eqs 6 and 7 and the dependence of $\Delta G'^{\ddagger}_{IU}$ is given by eqs 9 and 10.

RESULTS

Folding and Unfolding Kinetics of wt Barstar at 5 °C. Similar to the kinetics at 25 °C (Shastry *et al.*, 1994; Shastry & Udgaonkar, 1995) the observable kinetics of folding and unfolding of wt barstar at 5 °C are biphasic. The apparent rate constants of folding and unfolding, for both these phases at 5 °C, are depicted in Figure 2a,b. At 5 °C, the faster phase is about 3-fold slower and the slower phase is 10-fold slower than at 25 °C, at all GdnHCl concentrations. The resulting profile or the "Chevron plot" for the fast phase reveals a significant and abrupt reduction in slope, at and below 1.2 M GdnHCl concentration. Similar to the folding limb of the Chevron plot, the logarithm of the apparent unfolding rate also shows a curvature in its dependence on GdnHCl concentration (see Figure 2a and Discussion).

The apparent rates of folding and unfolding for the fast (λ_2) and the slow phase (λ_1) are seen to overlap in the range of GdnHCl concentration where they could both be measured. This indicates that these rates are independent of the starting conditions and depend only on the final conditions employed for unfolding (Figure 2a,b), as expected for a fully reversible process.

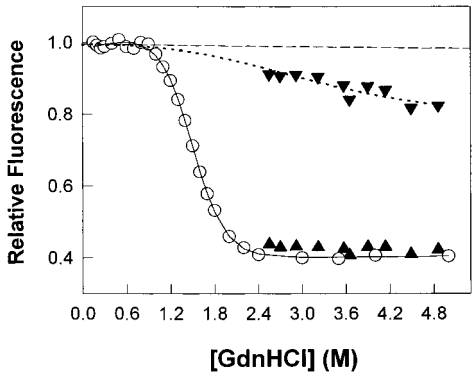

FIGURE 3: Kinetic and equilibrium amplitudes of the unfolding of wt barstar at pH 8, 25 °C. Unfolding was monitored by intrinsic tryptophan fluorescence (○) equilibrium unfolding curve; (▼) starting point of the kinetic unfolding curve, obtained by extrapolation to $t = 0$; (▲), end point of the kinetic unfolding curve, obtained by extrapolation to $t = \infty$. All amplitudes are relative to a value of 1 for F. The solid line is a fit of the equilibrium unfolding data to a two-state F ⇌ U transition. The midpoint of the equilibrium unfolding curve is 1.48 M. The dashed line is the estimated value of the optical signal of F obtained by linear extrapolation from the folded protein baseline. The dotted line has been drawn from a nonlinear least-squares fit, as described in the Results section. The values obtained for ΔG_{FI} and m_{FI} (ΔG_{FI}i) from this fit are 1.16 kcal·mol^{-1} and −0.49 kcal·mol^{-1}·M^{-1}, respectively.

Figure 2c shows the fractional amplitudes of the slower phase of folding and unfolding at 5 °C. There is a significant shortfall in the fractional unfolding amplitude *vis-a-vis* the fractional folding amplitude at 1.5 M GdnHCl. The mismatch is accentuated with a decrease in the GdnHCl concentration. This mismatch, seen only at 5 °C and not at 25 °C (Shastry *et al.*, 1994), might occur because the equilibrium constant governing the $U_F \rightleftharpoons U_S$ reaction is temperature-dependent. This was shown, however, not to be the case: when unfolded barstar (in 6 M GdnHCl) at either 0 or at 72 °C was diluted to 1.6 M GdnHCl at 25 °C, the rates as well as the fractional amplitudes of the resulting slow phases of folding, when monitored using the far-UV CD signal at 222 nm, did not differ (data not shown).

Burst-Phase Loss of Fluorescence at Low Temperatures. Figure 3 shows a superposition of the kinetic start and end points on the equilibrium unfolding curve of wt barstar at 5 °C. The midpoint of the equilibrium transition at 5 °C is 1.48 M GdnHCl, which is lower than the value of 1.9 M obtained at 25 °C. This shows that barstar is destabilized at 5 °C [also see Agashe and Udgaonkar, (1995)]. Figure 3 reveals that there is a burst-phase loss of fluorescence intensity during unfolding. The starting points of the unfolding kinetics deviate systematically below the extrapolated native baseline from the equilibrium denaturation curve. This deviation shows an increase with an increase in the GdnHCl concentration, reaching a value of ∼30% of the total change, in 5 M GdnHCl. The end points of the unfolding kinetics fall, however, on the unfolded protein baseline of the equilibrium curve, as expected. This confirms that in the concentrations of GdnHCl used for unfolding (2.6−5 M) there are no slow phases that contribute to the kinetics, and the burst phase together with the single observable phase accounts for the entire equilibrium unfolding amplitude. Thus, the data in Figure 3, obtained using fluorescence

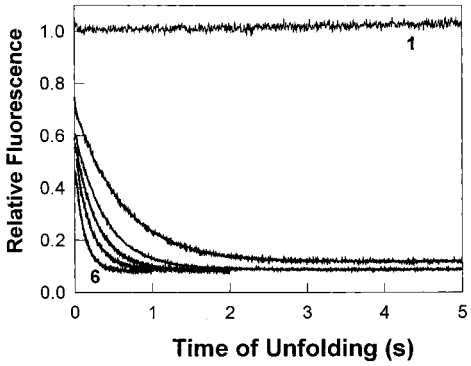

FIGURE 4: Fluorescence-monitored unfolding kinetics of W38FW44F at pH 8, 10 °C. Intrinsic tryptophan fluorescence was excited at 295 nm while the emission was set at 320 nm to monitor unfolding. Fluorescence values were normalized to that of the fully folded protein. The relative fluorescence so obtained is plotted against the time of unfolding. Trace 1 is the fully folded protein baseline and trace 6 is the unfolding curve in 5.8 M GdnHCl. The intervening traces represent unfolding in 3.0, 3.7, 4.2, and 4.8 M GdnHCl, in the order of their occurrence from top to bottom. Each kinetic trace shown represents the average of eight separately acquired traces.

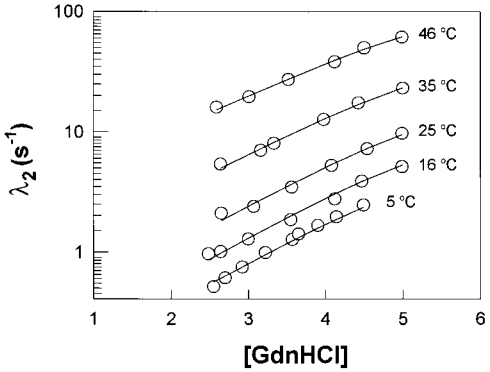

FIGURE 5: Dependency of the rate constant of unfolding of wt barstar on GdnHCl concentration and temperature at pH 8. Unfolding was monitored by intrinsic tryptophan fluorescence. The logarithm of the observed first-order rate constant of unfolding, λ_2, is plotted as a function of GdnHCl concentration and temperature. The solid lines through the data points were obtained from a kinetic modeling of the data to eq 11 and values at 25 °C for ΔH_{FI}, $T\Delta S_{FI}$, $\Delta C_{p,FI}$, ΔH_{FI}^{i}, $T\Delta S_{FI}^{i}$, $\Delta C_{p,FI}^{i}$, $\Delta H_{IU}^{\ddagger}$, $T\Delta S_{IU}^{\ddagger}$, $\Delta C_{p,IU}^{\ddagger}$, $\Delta H_{IU}^{\ddagger,i}$, $T\Delta S^{\ddagger,i}{}_{IU}$ and $\Delta C_{p,IU}^{\ddagger,i}$ of 3.94 kcal.mol^{-1}, −0.06 kcal.mol^{-1}, 0 kcal·mol^{-1}·K^{-1}, −0.91 kcal·mol^{-1}·M^{-1}, −0.24 kcal·mol^{-1}·M^{-1}, 0 kcal·mol^{-1}·K^{-1}.M^{-1}, 11.25 kcal.mol^{-1}, −3.11 kcal.mol^{-1}, 0.65 kcal·mol^{-1}·K^{-1}, 0.3 kcal·mol^{-1}·M^{-1}, 0.12 kcal·mol^{-1}·M^{-1} and −0.06 kcal·mol^{-1}·K^{-1}·M^{-1}, respectively.

intensity to monitor unfolding, complement the observed occurrence of I_U, inferred from far-UV CD monitored unfolding kinetics at 25 °C (Nath *et al.*, 1996).

The dotted line in Figure 3 represents a nonlinear least-squares fit of the GdnHCl concentration dependence of the accumulation of I_U to a two-state (see Data Analysis) F ⇌ I_U transition. To do so, it was assumed that the slopes of the intermediate and unfolded protein baselines were identical. Since the true spectroscopic properties of I_U in comparison to the folded and the unfolded states are not known, it must be stressed that such a procedure provides only gross estimates for the values of ΔG_{FI} and, in particular, m_{FI} (ΔG_{FI}^{i}). The estimates obtained for these quantities are given in the legend to Figure 3 and served as initial estimates for these parameters in the kinetic modeling of the data in Figure 5 to eq 11 (see Discussion).

The ∼30% burst-phase loss in fluorescence during unfolding in 5 M GdnHCl at 5 °C is less than the ∼50% contribution seen during far-UV CD-monitored unfolding in 5 M GdnHCl at 25 °C (Nath *et al.*, 1996). To confirm the authenticity of the burst-phase fluorescence loss during the unfolding of wt barstar, the unfolding of the W38FW44F mutant of barstar was studied at 10 °C. The W38FW44F mutant has a single tryptophan at position 53, is marginally unstable compared to the wild-type protein, and has been shown to unfold via I_U at 25 °C, as does wt barstar (Nath *et al.*, 1996). W38FW44F shows a much greater percentage change in fluorescence intensity on unfolding, and its kinetics are simpler to interpret in terms of burial or exposure of the single indole fluorophore, which reports on the formation or disruption of the hydrophobic core (Nath & Udgaonkar, 1997). Figure 4 shows the unfolding curves of W38FW44F at 10 °C, at various GdnHCl concentrations. With respect to the native fluorescence intensity, it is seen that there is an increasing burst-phase loss of fluorescence in increasing concentrations of GdnHCl. The starting values of the unfolding curves are therefore progressively lower when increasing concentrations of GdnHCl are used for unfolding. The burst-phase loss with respect to the native state fluorescence and as a fraction of the total observed change attains a value of ∼55% in 5 M GdnHCl. This change is substantially higher than that for the wild-type protein at 5 °C but is comparable to the burst-phase change in far-UV CD-monitored unfolding in 5 M GdnHCl at 25 °C (Nath *et al.*, 1996). As shown in Figure 4, the expected increase in the unfolding rates with an increase in the GdnHCl concentration is seen.

Temperature Dependence of Unfolding Kinetics. The apparent rates of GdnHCl-induced unfolding of wt barstar were measured at six different concentrations of GdnHCl in the range 2.6−5 M, at five different temperatures from 5 to 46 °C. The slow phase of unfolding that is seen in the unfolding transition zone of an equilibrium unfolding curve, which corresponds to the U_F ⇌ U_S reaction, becomes negligible (< 2%) above 2.6 M GdnHCl (the lowest concentration of GdnHCl used) at all temperatures from 5 to 46 °C; thus, only a single-exponential fast phase of unfolding is seen. The apparent rates of unfolding, λ_2, so determined are shown in Figure 5. A plot of the logarithm of λ_2 versus GdnHCl concentration shows a perceptible curvature at 5 °C (see Discussion), while the plots at higher temperatures appear more linear.

The dependence of the observed rate constants, on temperature as well as GdnHCl concentration, is described by eq 11. Equation 11 contains 12 independently variable parameters. Of these, six are the enthalpy, the entropy, and the heat capacity terms for the two unfolding steps, F ⇌ I_U and I_U ⇀ TS (three each), and the remaining six are the interaction terms that govern the dependences of these parameters on GdnHCl concentration. The values of the 12 parameters are subject to only two reasonable constraints: (1) the values of ΔG_{FI} ($\Delta H_{FI} - T\Delta S_{FI}$) and ΔG_{FI}^{i} ($\Delta H_{FI}^{i} - T\Delta S_{FI}^{i}$) at 5 °C are constrained (within a margin of error of 50%) to values determined from a two-state F ⇌ I_U fit of the dependence of the burst-phase amplitudes on GdnHCl concentration (see Results) and (2) the value of $\Delta C_{p,FI} + \Delta C_{p,IU}^{\ddagger}$ is constrained to a value less than that of $\Delta C_{p,FU}$, the total change in heat capacity upon complete unfolding of F to U, whose value (1500 kcal·mol^{-1}·K^{-1}) is accurately known from earlier work (Agashe & Udgaonkar, 1995;

Wintrode *et al.*, 1995). With these constraints, the data in Figure 5 could be fit well to eq 11, and the values obtained for the 12 parameters are listed in the legend to Figure 5. There are, however, too many variable parameters in eq 11 for these values to be accepted as reliable and accurate, because of the well-known problem of multiple minima.

Of principal interest was whether upper and lower bounds for $\Delta C_{p,FI}$ and $\Delta C_{p,IU}^{\ddagger}$ could be determined. Kinetic modeling of the data to eq 11 was therefore carried out using computer simulations, in which $\Delta C_{p,FI} + \Delta C_{p,IU}^{\ddagger}$ was fixed to different values between 0 and 1500 at intervals of 50. For each fixed value of $\Delta C_{p,FI} + \Delta C_{p,IU}^{\ddagger}$, the values of the 12 parameters were varied within the two constraints described above. When $\Delta C_{p,FI} + \Delta C_{p,IU}^{\ddagger}$ was fixed to a value below 550 or above 750, the kinetic modeling did not simulate the data well. Values for $\Delta C_{p,FI} + \Delta C_{p,IU}^{\ddagger}$ fixed between 550 and 750 resulted in the best and satisfactory simulations and suggested values for $\Delta C_{p,FI}$ between 0 and 15. If the value of $\Delta C_{p,FI}$ was forced to be greater than 50, the simulations did not model the data well. Small changes in $\Delta C_{p,FI} + \Delta C_{p,IU}^{\ddagger}$ in the simulations lead to very large changes in the values for the eight enthalpy and entropy parameters of eq 11. Thus, the kinetic modeling suggests that the change in heat capacity upon activation of the fully folded protein to the transition state, given by $\Delta C_{p,FI} + \Delta C_{p,IU}^{\ddagger}$, has a value of 650 ± 100 cal.mol^{-1}·K^{-1}, and that the contribution of $\Delta C_{p,FI}$ to this quantity is negligible.

DISCUSSION

Folding Kinetics at 5 °C. The logarithm of the apparent folding rate at 5 °C shows a change in the slope of its dependence on GdnHCl concentration (Figure 2a), referred to as a "roll over" by Baldwin (1996). It suggests a change in the folding mechanism at concentrations of GdnHCl lower than 1.2 M. Such behavior has been attributed previously to the appearance of a very early intermediate in the case of ubiquitin (Khorasanizadeh *et al.*, 1996) and barnase (Matouschek *et al.*, 1990). A very early intermediate lacking optically active structure (Shastry & Udgaonkar, 1995; Agashe *et al.*, 1995), I_{M1}, has been shown to accumulate on the major folding pathway of barstar, $U_S \rightarrow I_{M1} \rightarrow I_{S1} \rightarrow I_N \rightarrow F$. There is, however, no distinct "roll over" apparent in the folding kinetics of barstar at 25 °C (Shastry & Udgaonkar, 1995). At 5 °C, the relative concentration independence of the folding rate below 1.2 M GdnHCl may occur due to a change in the structure and hence the position of the transition state of folding on the reaction pathway (Roder & Colón, 1997). Roder and Colón have reasoned that if the folding transition state is very similar to the preceding intermediate in its solvent accessibility then the kinetic *m*-value, $m^{\ddagger}$, given by the GdnHCl concentration dependence of the folding rate should be negligibly small (Roder & Colón, 1997). Multiple pathways and intermediates make the analysis of the transition state of folding of barstar very complex, and consequently, at present, a more detailed investigation of this state has been omitted. The exact reasons for the observed "roll over" are therefore unclear and the explanation offered here is merely speculative.

Unfolding Kinetics at 5 °C. The biphasic nature of the observable folding and unfolding kinetics of barstar at 25 °C is preserved in the observable kinetics at 5 °C as well. The slow-phase amplitudes from the folding and unfolding experiments overlap completely at 25 °C. According to the extended two-state model of folding, $F \rightleftharpoons U_F \rightleftharpoons U_S$, if the equilibrium constant for the $U_F \rightleftharpoons U_S$ transition, K_{21}, is independent of GdnHCl concentration, then the slow-phase amplitudes from folding and unfolding experiments should be identical under identical conditions (Shastry *et al.*, 1994). In a control experiment K_{21} was also seen to be temperature-independent (see Results). Consequently, if the $F \rightleftharpoons U_F \rightleftharpoons U_S$ model is followed at 5 °C, the slow-phase amplitudes should overlap completely at this temperature as well. The observed mismatch between the folding and unfolding amplitudes of the slow phase is contrary to this expectation. It suggests that the folding mechanism at 5 °C is more complex than this simple scheme. A plausible explanation for this behavior at 5 °C could be the observed presence of an intermediate, I_U, on the unfolding pathway (see Results and Figure 3) in a GdnHCl concentration-dependent manner. The mismatch could arise, for instance, from a kinetic coupling between the $I_U \rightharpoonup U$ step and the $F \rightleftharpoons I_U$ preequilibrium during unfolding.

The unfolding limb of the Chevron plot (Figure 2a) also appears to be nonlinear. Such nonlinearity has also been seen in the case of barnase (Matouschek & Fersht, 1993; Matouschek *et al.*, 1994) and the Arc repressor (Jonsson *et al.*, 1996). In the latter case, the nonlinearity has been interpreted to result from the accumulation of kinetic intermediates on the unfolding pathway, and a change in the unfolding mechanism at higher concentrations of GdnHCl, but no direct evidence for kinetic unfolding intermediates was available. In contrast, at least one kinetic unfolding intermediate has been implicated directly on the unfolding pathway of barstar (Nath *et al.*, 1996; see also below).

Burst-Phase Fluorescence Loss at 5 °C. Data presented here show (Figure 3) that at 5 °C, there is a very rapid loss of intrinsic Trp fluorescence intensity during unfolding of wt barstar. The W38FW44F mutant also displays a more pronounced burst-phase change (Figure 4) even at a higher temperature of 10 °C. Earlier results had shown that the intrinsic Trp fluorescence intensity does not report on structural changes during the burst-phase of unfolding at 25 °C (Nath *et al.*, 1996). The observation holds true for both the wild-type and the W38FW44F mutant of barstar although there are substantial, concomitant burst-phase losses in the secondary structure during unfolding. The observation of a burst-phase change in fluorescence only at low temperature suggests that hydrophobic interactions are weakened at 5−10 °C, resulting in the hydrophobic core of I_U being less compact and therefore less sequestered from water than it is at 25 °C.

At lower temperatures, weakening of the hydrophobic forces that stabilize the protein at room temperature is expected because an increased hydration of nonpolar surfaces is favored, while at 25 °C, the hydration of nonpolar surfaces is not favorable (Privalov, 1992; Agashe & Udgaonkar, 1995). Barstar undergoes very pronounced cold denaturation that is strongly accentuated by the presence of GdnHCl (Agashe & Udgaonkar, 1995). The results suggest that I_U probably undergoes even more pronounced cold denaturation. Thus, partial hydration of the hydrophobic core of I_U occurs at low temperatures but not at high temperatures. Complete hydration of the hydrophobic core occurs only in the rate-limiting step. Hence, most of the native fluorescence

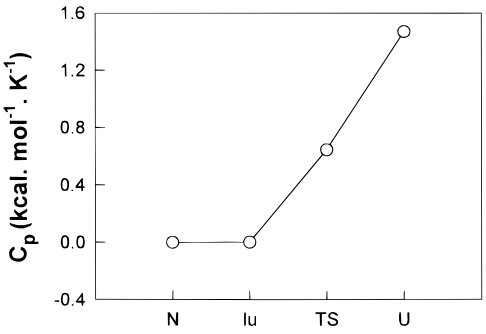

FIGURE 6: Change in heat capacity along the reaction profile for the unfolding of wt barstar at pH 8, 25 °C, 0 M GdnHCl. The reaction coordinate is the unfolding pathway: F → I_U → TS → U_F. The F state has been assigned, arbitrarily, a value of 0.

intensity of the wild-type protein is lost only during the rate-limiting step.

Heat Capacity Changes during Unfolding. The known occurrence of an unfolding intermediate at 25 °C, and added evidence for its presence at 5 °C, using fluorescence as a probe, prompted a three-state, F ⇌ I_U ⇀ U, analysis of the unfolding kinetics. Since there were too many parameters to fit directly the data to eq 11, kinetic simulations were carried out using eq 11 to determine whether the values for $\Delta C_{p,FI}$ and $\Delta C_{p,IU}^{\ddagger}$, could be determined. These simulations suggest that the heat capacity increment in going from the F to the TS state appears to occur exclusively in the I_U → TS step (Figure 6). Consequently, I_U appears to have a heat capacity indistinguishable from that of F.

It was previously inferred from the spectroscopic features of I_U that it is a compact intermediate which has lost a considerable amount of the native secondary structure and yet has a hydrophobic core that is not hydrated at room temperature. The absence of a change in the heat capacity, ΔC_p, in the F ⇀ I_U step supports the earlier findings of Nath *et al.* (1996) that I_U resembles F in terms of the exposed surface area. The contributions to ΔC_p are complex in nature and are not exclusively due to the exposure of nonpolar surface area (Privalov, 1992; Spolar *et al.*, 1992). It is prudent, therefore, not to interpret this value as a quantitative estimate of the nonpolar surface area exposed by I_U, *vis-a-vis* the F state, but only as a gross indicator of its degree of compactness. It is safe to conclude that I_U is as compact as F.

The unfolding reaction proceeds beyond I_U with a cooperative loss of secondary and tertiary structure as monitored by far-UV CD and fluorescence, respectively (Nath *et al.*, 1996). The transition state of this step is also the rate-limiting step for the entire unfolding transition. Figure 6 indicates that the TS has a value for ΔC_p that is ∼45% higher than that of F. The transition state of unfolding is therefore ∼55% nativelike by the ΔC_p criterion. The position of the unfolding transition state on the reaction coordinate with respect to the F and the U states is therefore roughly in the middle by this criterion. Segawa and Sugihara (1984) found the folding transition state of disulfide-intact hen lysozyme to possess a completely nativelike heat capacity. T4 lysozyme, on the other hand, was shown to be 75% nativelike in its heat capacity (Chen *et al.*, 1989, 1992). Chymotrypsin inhibitor 2 (CI2) shows a very small change in heat capacity during the transition from U to the transition state (Oliveberg *et al.*, 1995). This suggests that the folding transition state of CI2 is closer to the unfolded state than the folded state (Itzhaki *et al.*, 1995). Cold shock protein B (Csp B) was recently shown to have a transition state that is 90% nativelike (Schindler & Schmid, 1996), and that of the α subunit of tryptophan synthase was shown to be practically identical to the F state (Chen & Matthews, 1994) by the ΔC_p criterion.

In conclusion, the fluorescence-monitored unfolding experiments at low temperature reported here have confirmed the previous demonstration by far-UV CD measurements at 25 °C of the accumulation of the unfolding intermediate I_U on the unfolding pathway. At low temperature, the hydrophobic core of I_U is partially solvated by water, but complete penetration of water into the core occurs concurrently with loss of all structure only during the rate-limiting step of unfolding. A thermodynamic analysis of the unfolding kinetics confirms the nativelike compactness of I_U and has provided further insight into the properties of the transition state of unfolding. Finally, a relative lack of unfolding studies with multiple structural probes might be responsible for the belief that unfolding kinetics are always simple and monophasic.

ACKNOWLEDGMENT

V.R.A. acknowledges the receipt of a fellowship from the Deutscher Akademischer Austauschdienst (DAAD) for the duration of his stay in Bayreuth and Thomas Schindler for help in conducting the stopped-flow experiments at low temperature. We thank Utpal Nath for his help with the simulations, for discussions, and for his comments on the manuscript.

REFERENCES

Agashe, V. R., & Udgaonkar, J. B. (1995) *Biochemistry 34*, 3286−3299.
Agashe, V. R., Shastry, M. C. R., & Udgaonkar, J. B. (1995) *Nature 377*, 754−757.
Atkins, P. W. (1978) *Physical Chemistry*, W. H. Freeman & Co., San Francisco.
Baldwin, R. L. (1996) *Fold. Des. 1*, R1−R8.
Chen, B. L., Baase, W. A., & Schellman, J. A. (1989) *Biochemistry 28*, 691−699.
Chen, B. L., Baase, W. A., Nicholson, H., & Schellman, J. A. (1992) *Biochemistry 31*, 1464−1476.
Chen, X. W., & Matthews, C. R. (1994) *Biochemistry 33*, 6356−6362.
Fersht. A. R. (1995a) *Curr. Opin. Struct. Biol. 5*, 79−84.
Fersht, A. R. (1995b) *Philos. Trans. R. Soc. London B: Biol. Sci. 348*, 11−15.
Hänggi, P., Talkner, P., & Borkovec, M. (1990) *Rev. Mod. Phys. 62*, 251−341.
Hoeltzli, S. D., & Frieden, C. (1995) *Proc. Natl. Acad. Sci. U.S.A. 92*, 9318−9322.
Itzhaki, L. S., Otzen, D. E., & Fersht, A. R. (1995) *J. Mol. Biol. 254*, 260−288.
Jonsson, T., Waldburger, C. D., & Sauer, R. T. (1996) *Biochemistry 35*, 4795−4802.
Khorasanizadeh, S., Peters, I. D., & Roder, H. (1996) *Nat. Struct. Biol. 3*, 193−205.
Khurana, R., & Udgaonkar, J. B. (1994) *Biochemistry 33*, 106−115.
Khurana, R., Hate, A. T., Nath, U., & Udgaonkar, J. B. (1995) *Protein Sci. 4*, 1133−1144.
Kiefhaber, T., Labhardt, A. M., & Baldwin, R. L. (1995) *Nature 375*, 513−515.
Kraulis, P. (1981) *J. Appl. Crystallogr. 24*, 946−950.
Lubienski, M. J., Bycroft, M., Freund, S. M. V., & Fersht, A. R. (1994) *Biochemistry 33*, 8866−8877.

Matouschek, A., & Fersht, A. R. (1993) *Proc. Natl. Acad. Sci. U.S.A. 90*, 7814−7818.
Matouschek, A., Kellis, J. T., Jr., Serrano, L., & Fersht, A. R. (1989) *Nature 342*, 122−126.
Matouschek, A., Kellis, J. T., Jr., Serrano, L., Bycroft, M., & Fersht, A. R. (1990) *Nature 346*, 440−445.
Matouschek, A., Matthews, J. M., Johnson, C. M., & Fersht, A. R. (1994) *Protein Eng. 7*, 1089−1095.
Nath, U., & Udgaonkar, J. B. (1997) *Biochemistry 36*, 8602−8610.
Nath, U., Agashe, V. R., & Udgaonkar, J. B. (1996) *Nat. Struct. Biol. 3*, 920−923.
Nölting, B., Golbik, R., & Fersht, A. R. (1995) *Proc. Natl. Acad. Sci. U.S.A. 92*, 10668−10672.
Nölting, B., Golbik, R., Neira, J. L., Soler-Gonzalez, A. S., Schreiber, G., & Fersht, A. R. (1997) *Proc. Natl. Acad. Sci. U.S.A. 94*, 826−830.
Oliveberg, M., Tan, Y. -J., & Fersht, A. R. (1995) *Proc. Natl. Acad. Sci. U.S.A. 92*, 8926−8929.
Privalov, P. L. (1992) in *Protein Folding*, (Creighton, T. E., Ed.) W. H. Freeman & Co., New York.
Roder, H., & Colón, W. (1997) *Curr. Opin. Struct. Biol. 7*, 15−28.
Schellman, J. A. (1987) *Biopolymers 7*, 1305−1322.
Schindler, T., & Schmid, F. X. (1996) *Biochemistry 35*, 16833−16842.
Schreiber, G., & Fersht, A. R. (1993) *Biochemistry 32*, 11195−11203.
Segawa, S., & Sugihara, M. (1984) *Biopolymers 23*, 2473−2488.
Shastry, M. C. R., & Udgaonkar, J. B. (1995) *J. Mol. Biol. 247*, 1013−1027.
Shastry, M. C. R., Agashe, V. R., & Udgaonkar, J. B. (1994) *Protein Sci. 3*, 1409−1417.
Spolar, R. S., Livingstone, J. R., & Record, M. T., Jr. (1992) *Biochemistry 31*, 3947−3955.
Wintrode, P. L., Griko, Y. V., & Privalov, P. L. (1995) *Protein Sci. 4*, 1528−1534.

BI971062D